A Novel, Low-Cost, High-Performance Single-Phase Adjustable-Speed Motor Drive Using PM Brush-Less DC Machine: IIT's Design for 2003 Future Energy Challenge

Aly A. Aboulnaga, Piyush C. Desai, Fernando Rodriguez, Timothy R. Cooke, and Ali Emadi
Grainger Power Electronics and Motor Drives Laboratory
Electric Power and Power Electronics Center
Illinois Institute of Technology
Chicago, IL 60616-3793, USA
Phone: +1/(312)567-8940; Fax: +1/(312)567-8976
E-mail: emadi@iit.edu

***Abstract*—This paper presents a novel, low-cost, high-performance single-phase adjustable-speed motor drive by using a three-phase permanent magnet brush-less DC (BLDC) machine. This system has been designed and implemented by the multi-disciplinary student team of Illinois Institute of Technology (IIT) for the 2003 IEEE/DOE/DOD International Future Energy Challenge and won the First Prize Overall Award for the Motor Competition. Machine configurations and driver topologies have been investigated to develop a low-cost innovative system. To satisfy the requirements of the challenge, a commercially available motor has been selected and re-designed including the stator winding and permanent magnet rotor. The re-designed motor has been fabricated and tested successfully. For the designed power electronic driver, the main goal was to achieve high performance and reliability at low cost. Simulation and experimental results are provided to verify the proposed approach.**

I. Introduction

As environmental and other concerns slow the growth of electrical energy generation in coming years, it becomes essential that we conserve and use this limited and precious resource more efficiently. Conserving electricity and making it a better fuel relies on the widespread adoption of the power conversion process, which takes electricity from a source and converts it to a form exactly suited to the electrical load.

Electric motors consume more than 75% of all electrical power in the United States. Adjustable-speed motors can improve the efficiency of these motors by about 50% in many applications. They can also reduce costs considerably. Power electronics allows us to develop efficient speed and torque control of electric motors at low costs. This, in turn, calls for development of optimized electro-mechanical power conversion units.

In this project, we have developed a novel, low-cost, high-performance single-phase adjustable-speed motor by using a three-phase permanent magnet brush-less DC (BLDC) machine. Machine configurations and driver topologies have been investigated to develop a low-cost innovative system. We have selected a motor from Poly-Scientific, which has been available in our lab. To satisfy the requirements of the challenge, we have re-designed the motor including the stator winding and permanent magnet rotor. Using the machine manufacturing facility at MPC Products Corporation and Mills Electric Company, we have fabricated the re-designed motor. The new motor has been tested successfully. Based on the re-designed machine, the team has worked with Infranor Inc. for the final machine for the competition. This machine is presented for the final testing.

Motor drive power converters, present poor power factor loads to the utility power systems. As a result, more generation and transmission capacity is needed to deliver the same amount of energy to the user. This, in turn, results in excessive energy losses in the form of copper losses. Considering the wide range of applications in motor drive market, development of high power quality conversion units becomes an essential necessity.

In this project, we have also developed a novel system with high power factor that is simple and low cost. We have also reduced system in-rush currents associated with motor starting and enhanced motor efficiency across a wide load range. The burden has been shifted to the complexity of control, which translates to more sophisticated, yet cheap, control integrated circuits (ICs). In order to achieve a very low cost drive, we have not used any digital signal processor, microprocessor, or microcontroller. Instead, we have investigated many available motor drives in the market and examined many control ICs, which are very cheap. We have been able to successfully develop the system meeting the requirements of the challenge using several ICs. This, in turn, has significant advantages for mass production because of economical development, simplicity, reliability, and ease of manufacturing. With the success of this concept, adjustable-speed motors have a better chance to penetrate the electric motor applications market. This, in turn, will fulfill the promise of significant saving in motor related energy consumption, without its adverse impact on the utility power systems.

Target hardware cost is US$40 for a combination of motor and motor controller that can operate from a single-phase residential source (220V, 60Hz), deliver rated shaft load of 3/4 HP (or 500 W) at 1500 RPM, exhibit a useful speed control range of at least 150 RPM to 5000 RPM, and provide power efficiency of at least 70% for loads ranging from 50 W to 500 W at a specified speed. In this paper, simulation and experimental results are provided to verify the novel design of the student team.

0-7803-8269-2/04/$17.00 (C) 2004 IEEE.

II. PERMANENT MAGNET BRUSH-LESS DC MACHINE DESIGN

A trapezoidal type BLDC machine has been designed and fabricated. In this machine, back-emf waveform is trapezoidal and is generated by trapezoidal air gap flux distribution and the machine has a trapezoidal or simple concentrated winding distribution over the stator periphery. For ripple free developed torque, the machine should be supplied by trapezoidal current waveforms. This requires low-resolution rotor position sensor such as hall-effect sensor, optical sensor fixed on rotor.

Motor terminal voltage for a three-phase full bridge inverter with six switches and Y-connected motor can be expressed as,

$$V_{DC} = E_f + 2\,R\,i_a + 2\,L\,\frac{di_a}{dt} \tag{1}$$

Assuming switches to be ideal, and emf between conducting phases to be constant (trapezoidal emf), the instantaneous armature current can be written as,

$$i_a(t) = \frac{V_{DC} - E_F}{2\,R}\left(1 - e^{\frac{(R)}{(L)}t}\right) + I_0 e^{\frac{(R)}{(L)}t} \tag{2}$$

We can express emf simply as a function of the rotor speed,

$$E_f = k_e\,n \tag{3}$$

Torque equation is similar to a conventional DC commutator motor and can be written as,

$$T_d = k_t\,i_a \tag{4}$$

The average developed torque can be maximized and torque ripple can be minimized if the emf waveform has a trapezoidal waveform. Trapezoidal waveform can be achieved by switching the MOSFETs or IGBTs in such a way that two-phase windings are always connected in series during whole conduction period of 60 degrees. In addition, proper shaping and magnetizing the permanent magnets and stator windings are important factors to obtain trapezoidal waveform. Owing to manufacturing tolerances, armature reactions, and other parasitic effects, EMF waveform is never ideally flat.

The volume of all permanent magnets used in a motor can be expressed as $V_m = 2\,p\,h\,w\,l$, where p is number of poles, and h, w, and l are height, width, and length of the PM, respectively. The output power of a PM machine is proportional to volume and quality of PM and maximum electromagnetic power developed by a PM machine can be expressed as (using operating diagram of PM material),

$$P_{\max} = \frac{\pi^2}{2}\frac{\xi}{k_f\,k_{ad}\,(1+\varepsilon)}\,f\,B_r H_c V_m \tag{5}$$

The apparent electromagnetic power crossing the air gap is,

$$S_{elm} = 0.5\,\pi^2\,k\,D^2\,L_i\,n_s\,B_g\,A_m \tag{6}$$

and the output power coefficient is,

$$\sigma_p = 0.5\,\pi^2\,k\,A_m\,B_g\,\eta\,Cos\phi \tag{7}$$

The air gap magnetic flux density,

$$B_g = \frac{\Phi_f}{\alpha_i\,\tau\,L_i} \tag{8}$$

For sizing procedure of NdFeB PM machines can initially be estimated as $B_g \approx (0.7\ldots0.9)B_r$. The magnetic flux density can also be approximately estimated on the basis of

$$B_g \approx \frac{B_r}{1 + \frac{\mu_{rrec}\,g}{h}} \tag{9}$$

There is a free choice in the effective length of the armature stack, i.e., ratio of L_i/D depends on the motor application. The air gap is advised to be 0.3 to 1.0 mm for small PM machines. The smaller the air gap, the lower the starting current. However, smaller air gap tends to increase the effect of armature reaction and detent torque.

Permanent magnet brush-less DC motors predominantly have surface-mounted magnet rotors with large effective pole-arc coefficients. For an ideal rectangular distribution of air gap magnetic flux density B_g=constant in the interval of $0 \le x \le \tau$, where τ is pole pitch, or from 0 to 180 degrees,

$$\Phi_f = L_i \int_0^{\tau} B_g\,dx = \tau\,L_i\,B_g \tag{10}$$

Including the pole shoe width $b_p < \tau$ and a fringing flux, the EMF contributing to the to the electromagnetic power is,

$$E_f = 8\,p\,N\,k\,\alpha_i\,\tau\,L_i\,B_g\,n \tag{11}$$

The electromagnetic torque developed by the motor is,

$$T_d = \frac{4}{\pi}\,p\,N\,k\,\alpha_i^{(sq)}\,\tau\,L_i\,B_g\,n \tag{12}$$

Power density and torque density are the measures to judge how best the active materials of a BLDC motor are utilized. NdFeB magnets offer the highest energy density at reasonable costs. Their major drawback, compared to SmCo, is temperature sensitivity. When using NdFeB magnets, the motor's temperature must be kept below 170 degrees to 250 degrees. Since the rotor losses are small, passive cooling is employed for the rotor. The main dimensions (inner stator diameter and effective length of core) for the BLDC are determined by rated power output, air gap magnetic flux density, and armature line current, as described above.

The geometry of the designed motor is as shown in Figure 1. Using Maxwell 2D software package of Ansoft Corporation, the design was analyzed and various solutions have been obtained. The software generated initial mesh and then it was refined as per the requirement. Enlarged view of the final mesh is shown in Figure 2.

Solutions for the torque was obtained and compared to the challenge requirements. Design torque and torque obtained by finite element analysis were closely matched, which strengthened the design objective.

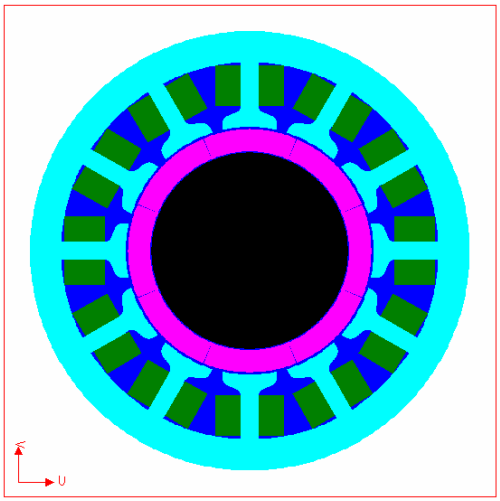

Figure 1. Geometry of the designed PM BLDC motor.

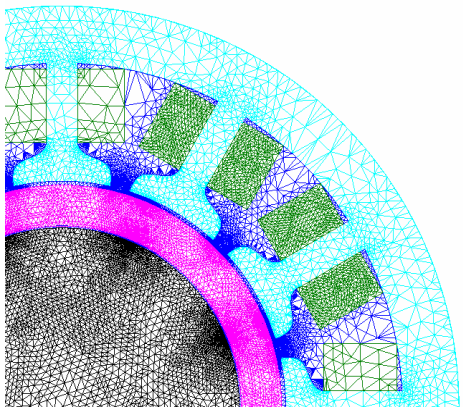

Figure 2. Enlarged view of the final mesh using Maxwell 2D.

Distribution of flux lines and magnetic flux density are shown in Figures 3 and 4.

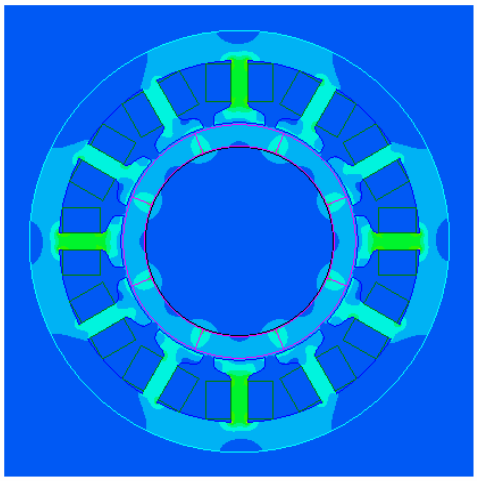

Figure 3. Magnetic flux density (designed motor).

Design parameters are chosen based on the analytical methodology as explained above. The design is verified by the finite element (FE) analysis using Maxwell 2D software package. The results of analytical methodology and FE analysis are closely matching. Therefore, it can be concluded that design is capable of giving optimum performance, which not only meets the minimum requirements, but also gives better operations. Experimental results support this conclusion.

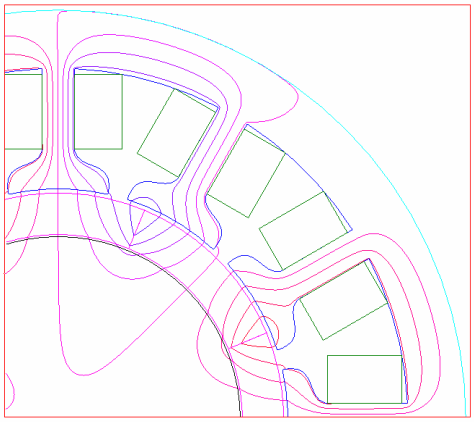

Figure 4. Distribution of flux lines (designed motor).

III. BLDC Drive Design

The permanent magnet brush-less DC motor shares the same torque speed characteristics and the basic operating principles of the brushed DC motor. The main difference is that the field windings are replaced by permanent magnets and the commutation is done electronically. Using PM and eliminating the brushes offer many distinctive advantages, such as high-performance torque control, low torque ripples, long life, high power to weight ratio, low noise and low EMI, better heat dissipation, low maintenance, and very high speed.

Our complete driving system has three main boards as follows:

- The AC/DC boost converter with power factor correction.
- The three-phase bipolar inverter circuit.
- The brush-less DC motor controller with closed loop feature.

Many ancillary factions have been added to assure reliable and efficient operation of the complete drive, such as over current protection, low voltage lockout, a complete isolation between the control circuit and the high voltage side of the inverter, and grounding of all metallic parts that do not belongs to the live circuit. The complete layout of the proposed PM BLDC drive is shown in Figure 5. The experimental set-up is shown in Figure 6.

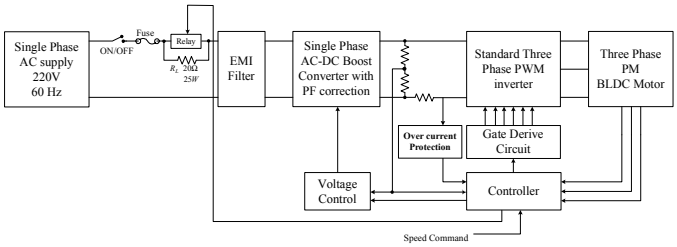

Figure 5. Layout of the permanent magnet brushless DC drive.

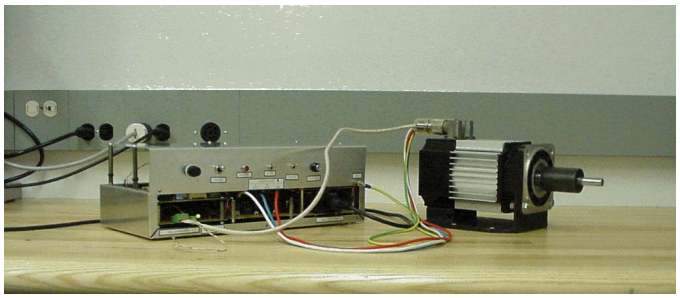

Figure 6. Developed PM BLDC adjustable-speed motor drive system.

A. AC/DC Boost Converter

To reach the desired high speed of the motor (5000rpm) and according to the back-emf sensitivity factor (0.75V/rpm), the DC link of the inverter should be fixed at 375V DC. To achieve this high DC link voltage from the main (220 VAC, 60Hz) along with high power factor and lower total harmonic distortion (THD) of the supply current, a boost converter is used. The boost converter, which operates in continuous conduction mode (CCM), offers an excellent choice to get the desired DC voltage with high power factor and near sinusoidal input current waveform. As shown in Figure 7, the AC/DC boost converter utilizes one bridge converter, one inductor, one MOSFET, one fast switching diode, and one bulk capacitor. Additional EMI filter is used at the input AC side to reduce EMI.

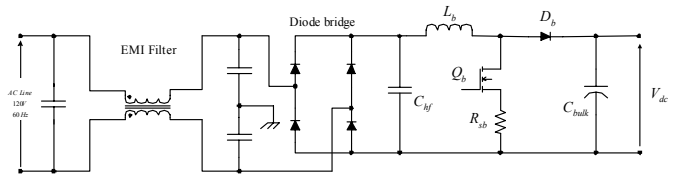

Figure 7. Circuit diagram of the boost converter.

To simply control the boost converter, NCP1650 is used. This new IC is an advanced IC for power factor correction that can operate over a wide range of input voltages and output power levels. It is designed to operate on 50/60 Hz power systems. This controller offers several different protection methods to assure safe, reliable operation under any conditions. The PWM is a fixed frequency, average current mode controller with a wide complement of features. These features allow for both flexibility as well as precision in its application to a circuit. Critical components of the internal circuitry are designed for high accuracy, which allows for precise power and current limiting, therefore, minimizing the amount of over design necessary for the power stage components. The NCP1650 is designed with a true power limiting circuit that will maintain excellent power factor even in constant power mode. It also contains features that allow for fast transient response to changing load currents and line voltages. The full feature of the used controller can be summarized as follows:

- Fixed frequency operation
- Average current mode PWM
- Continuous or discontinuous mode of operation
- Fast line/load transient compensation
- True power limiting circuit
- High accuracy multipliers
- Undervoltage lockout
- Overvoltage limiting comparator
- Ramp compensation does not affect oscillator accuracy
- Operation from 25 to 250 kHz

Protective features are: output voltage overshoot protection, low line input protection, instantaneous current limit, line frequency current limit, and maximum power limit.

In the power factor correction board, the switching frequency is set at 50 KHz. The used inductor is $150\mu H$. The used MOSFET is FDH27N50 with rated current of 27Amp and 500V and the used diode is STTA2006PI with rated current of 20Amp and 600V. The maximum power is set at 750W. In addition, three protective features are included: the first is a protection against over voltage runaway due to load removal, input under voltage lockout, cycle-by-cycle current limiting through a current limiting resistance, R_{sb}, and maximum power control. The achieved design provides a power factor of at least 0.95 through power rang of 100W up to the maximum power 750W.

B. Inverter

The used inverter is the standard bipolar three-phase one, which utilizes six MOSFETs arranged in three legs as shown in Figurer 8. The standard inverter is recommended for high power application (typically higher than 100W). The power MOSFET is selected because it is easy to drive, efficient, and inexpensive. The used power MOSFET is FDH27N50, which has a current rating of 27A and voltage rating of 500V and low on state resistance is 190mΩ. There are three attributes that make MOSFETs more reliable to be used in the BLDC inverter and other PWM systems. First, it can withstand high stress during commutations of the MOSFETs internal source drain diode. Second, MOSFETs are less susceptible to failure caused by brief drain-to-source over voltage transients. Third, MOSFETs have minimum gate-to-source rupture voltage ratings of 40V. A greater rupture voltage not only improves tolerance to electrostatic discharge and unanticipated gate-to-source voltage spikes, but it also extends the MOSFETs lifetime at all operating voltages. As the speed of the PM BLDC motor is proportional to the applied voltage, PWM control is used to control the effective DC link voltage over the armature windings. The theoretical waveforms of the PM BLDC and the phase currents are shown in Figurer 9.

For over current protection, sense resistance R_{si} is used. The sense voltage over R_{si}, which is proportional to the load current, is fed into a comparator on the main control board. The over current circuit limits the current not to exceed 140% of the rated current at the starting and in the case of overload. The designed value of R_{si} is 0.02Ω/3W.

C. Controller

The main duty of the brush-less DC motor controller is to decode the signals from the Hall effect sensors and generate correct logics to electronically commutate the motor. After comparing many brush-less DC motor controllers, we found

that the analog linear controller is very cheap, easy to implement, and requires fewer components along with high performance. The selected controller for the brush-less DC system highlighted here is built mainly with MC33035 and a closed loop adaptor chip, the MC33039. The two ICs are examples of many brush-less controller ICs that can be used to design a simple and low cost controller for the brush-less motors.

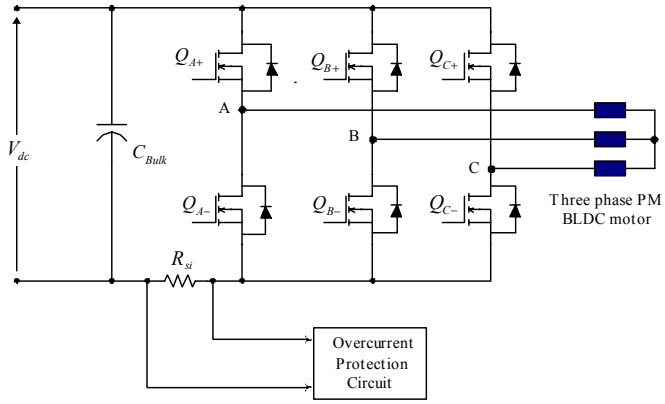

Figure 8. Three-phase unipolar inverter.

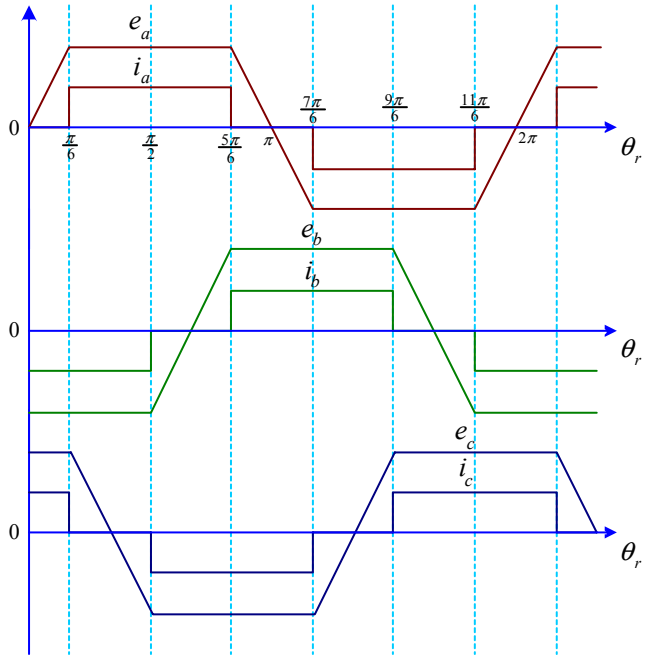

Figure 9. Ideal back-emf and phase current waveforms of the BLDC motor.

MC33035 is a 24-pin linear IC. It has an internal encoder, which decodes the signals from the Hall effect sensors and generates logic signals for proper switching sequence of the inverter switches. The generated commutation logic is internally fed into the six output drivers consisting of three open collector NPN transistors that drive the upper legs of the bridge and three totem pole drivers that control the devices. The open collector outputs can sink 50mA and the three lower totem pole outputs can source/sink 100mA.

To set the oscillator frequency, the values of timing components R_T and C_T are selected. From the MC33035's data sheet, the value of R_T and C_T are set to be 5.1kΩ and 9.1nF. This provides a nominal pulse width modulation frequency of 22 kHz, just above the audible range.

The speed can be changed from 0 rpm to the maximum speed (5000rpm) by changing the voltage of pin 11 from 0V to 3.25V. A potentiometer is connected to this pin to adjust its voltage when the maximum voltage of the speed command voltage is 10V. Additional resistance of 10Ω/0.5W and one diode and resettable fuse are connected in parallel with the potentiometer to avoided damage due to any accidental reversed polarity; this is completely illustrated in Figure 10.

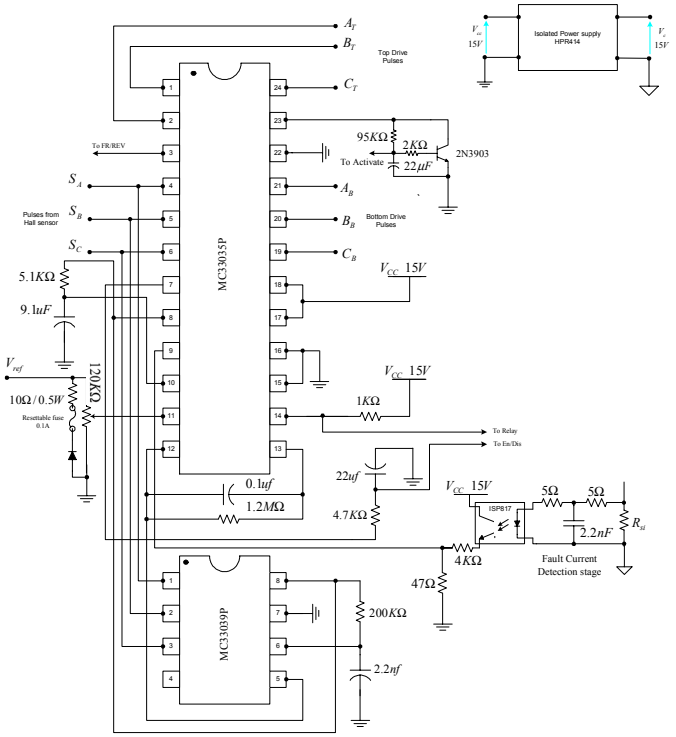

Figure 10. Closed loop control circuit for the BLDC drive.

The MC33035's circuitry contains one of the major elements for the closed loop speed control. The only piece lacking is one that monitors motor RPM and generates a signal proportional to the motor speed, a function that traditionally has been the domain of a tachometer. Once provided with a motor speed signal, the MC33035's high performance error amplifier and its internal oscillator form the last major links in the control loop. The closed loop adaptor, MC33039, is a low-cost, space saving IC. At each positive or negative transition of the Hall effect sensors, the MC33039 generates a pulse with a fixed on time. The output signal can then be filtered to obtain a voltage proportional to the motor speed. Design of the MC33035/MC33039-based system should begin with setting the system timing, which originates in the MC33039.

Selection of timing components for the MC33039 is based on the desired maximum motor RPM. Since our motor has four pairs of poles and three Hall sensors, for every mechanical revolution, each Hall-effect sensor delivers four pulses and the

three sensors generate twelve pulses. The MC33039 generates 24 pulses, one for each rising and falling edge. For a given maximum motor speed, the output pulse width has a maximum limit. As the maximum desired speed is 5000rpm, which is about 83 revolutions per second, the MC33039 will generate 83 x 24, or 2000 pulses per second. The 2 kHz frequency dictates that the maximum pulse width must be less than 0.5 mSec. From MC33039's data sheet, one can determine the values of the timing components *R* and *C* to be 200 kΩ and 2.2 nF, respectively. This results in a pulse width of 450us.

Both inputs and output of the MC33035's error amplifier are accessible to accommodate the control methods. This can be done by filtering the MC33039's output with a low pass filter to generate a voltage proportional to motor speed and feed the resulting signal into the inverting input of the MC33035's comparator. A signal proportional to desired motor speed drives the non-inverting input.

When motor speed falls below the desired speed, the MC33035 extends the output pulse width to the drive transistors. When motor speed is greater than the desired speed, the duty cycle decreases. The schematic of a closed loop brush-less motor control system is shown in Figure 10.

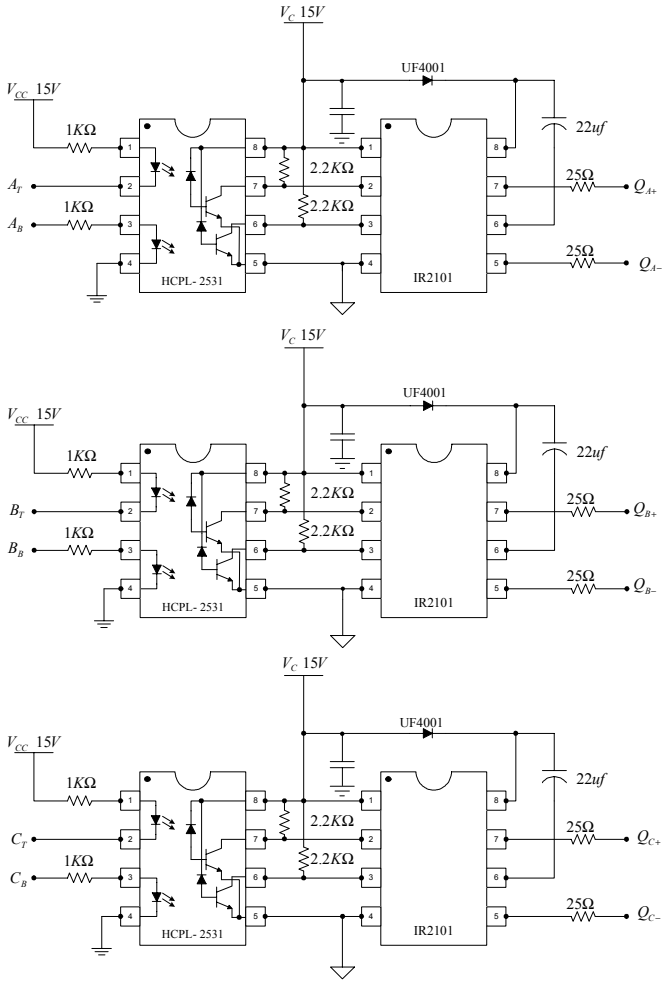

Figure 11. The driving stage (isolation between the control board and the power board).

In the main inverter circuits, there are six MOSFETs. Generally, the magnitude of the system voltage affects how one might deliver power to the MC33035 and generate the gate drive supply for the N-channel power MOSFETs. Here, the maximum applied voltage to the motor windings is 400V, since the MC33035 operates perfectly at a voltage between 10-20 V, it is desired to isolate the control board from the higher voltage of the power circuit. This can be done by using three high-speed dual-optocouplers (HCPL-2531) and three dual-gate drivers (IR2102); this is implemented as shown in Figure. 11.

To go for a more reliable solution, six optocouplers have been used along with six gate drivers. For the higher side switches, IR2118 is used as shown in Figurer. 12, while for the lower driver IR2125 is used. The IR2125 offers current detection and current limiting loop to limit driven power transistor current and programmable shutdown time. The protection circuitry of IR2125 detects over-current in the driven power transistor and limits the gate drive voltage. Cycle by cycle shutdown is programmed by an external capacitor, which directly controls the time interval between detection of the over-current limiting conditions and latched shutdown. The driving circuit for lower side MOSFETs is shown in Figure 13.

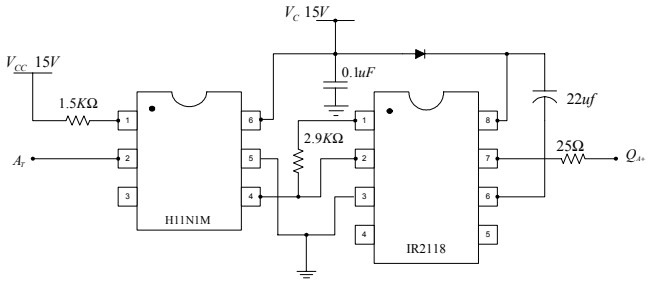

Figure 12. Driving circuit for the high side transistor.

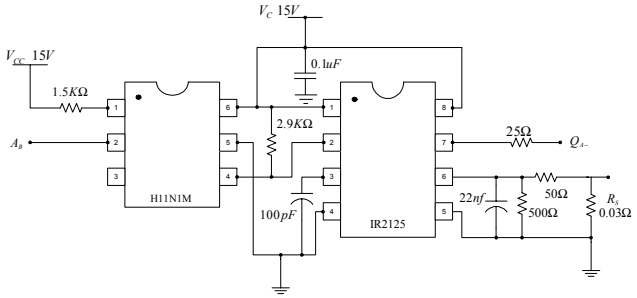

Figure 13. Driving circuit for the low side transistor.

The control board is supplied using step down transformer, bridge rectifier, and smoothing capacitor and voltage regulator as shown in Figure 14. An additional voltage regulator is used to maintain a constant 5V supply for the hall sensors. The power supply is protected at the secondary side of the transformer using a resettable fuse of 0.4A trip current.

There are many protective features of the controller; these futures can be summarized as follows:

Over-Current Protection: The over-current detection is achieved by sensing the voltage drop over the current sense resistor R_{si}. The sense voltage, which is proportional to the load

current, is fed into a comparator on board the MC33035. Once an over-current condition is detected, the output drivers turn-off the power MOSFETs in the remainder of the oscillator cycle. Because the isolation between the power circuit and the control circuit is necessary, the sense voltage on the current sense resistance is transmitted to the current sense terminal of the MC33035 through an optocoupler, as shown in Figure 10. Furthermore, the over-current protection is successfully done by IR2125, which has cycle-by-cycle current limiting and ability to shutdown the MOSFET when the time of the short circuit exceeds 1 uSec. Additionally, a fast acting fuse of 10A is used in the supply side to protect the whole drive boards from any accidental fault.

Under-Voltage Lockout: In addition to the over-current management, the MC33035 provides under-voltage lockouts that terminate the drive to the output transistors if any of the following three conditions occurs. The first is insufficient voltage to operate the IC. The second occurs when there is insufficient voltage to drive the power MOSFET gates. Finally, the output drivers turn off the power MOSFETs when the MC33035 does not sustain its on-board 6.25V reference.

Thermal Shutdown: Internal thermal shutdown circuitry is provided to protect the IC in the event the maximum junction temperature is exceeded. When activated, typically at 170°C, the IC acts as though the Output Enable was grounded.

Additional Features: Whenever a fault condition is present, an NPN transistor capable of sinking 16mA pulls the Fault Output pin (pin 14) low. Potential uses of the Fault Output include alerting a problem, lighting an LED, implementing a soft start feature to limit motor start up currents, or latching the system off at the first sign of a problem or after a fixed delay.

Grounding: To complete the security of the system, all the metallic parts that do not belong to the live parts as well as the body of the motor are connected to the ground.

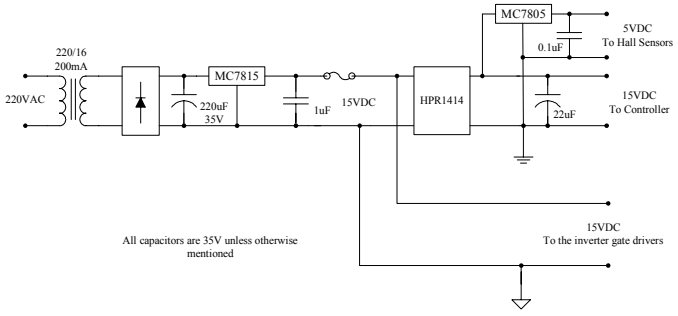

Figure 14. On-board power supply for the controller and the gate drivers.

IV. Simulation and Experimental Results

This section is mainly dedicated to present waveforms from the simulations and experimental models, to illustrate the complete operation of the drive. The following machine parameters are considered:

- Stator resistance: 2.4 Ω/phase
- Stator self-inductance: 4.8 mH/phase
- Stator mutual inductance: - 0.25 mH/phase
- Number of poles: 8
- Back-emf constant: 0.67V.s/rad
- Torque constant: 0.67N-m/A
- Rotor inertia: 500 mKg.m^2
- Mechanical time constant: 2.03 mSec.
- Electrical time constant: 2.00 mSec.
- Conduction pulse width for the driver: 120^o
- DC link voltage: 375V

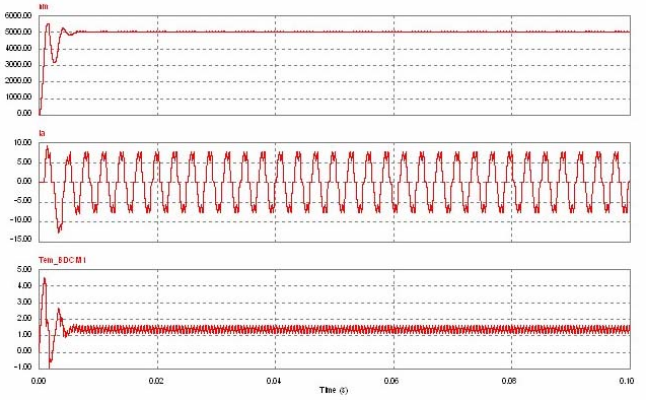

Figure 15. Motor simulation results at 5000rpm and 1.2 N-m average torque.

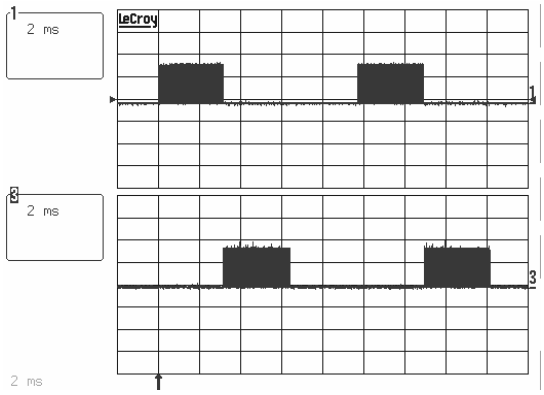

Figure 16. Driving pulses for (Q_{A-} and Q_{B-}), 10V/div; pulses generated from MC33035, motor speed: 1500rpm.

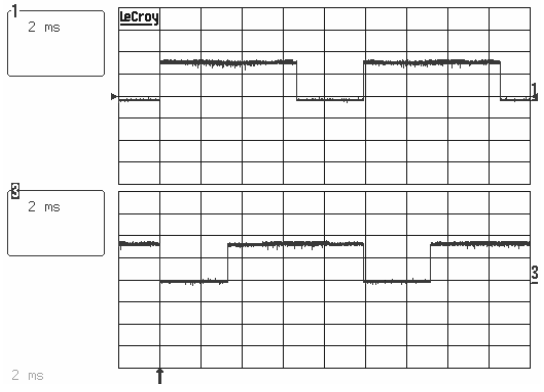

Figure 17. Inverted driving pulses for (Q_{A+} and Q_{B-}), 10V/div; pulses generated from MC33035, motor speed: 1500rpm.

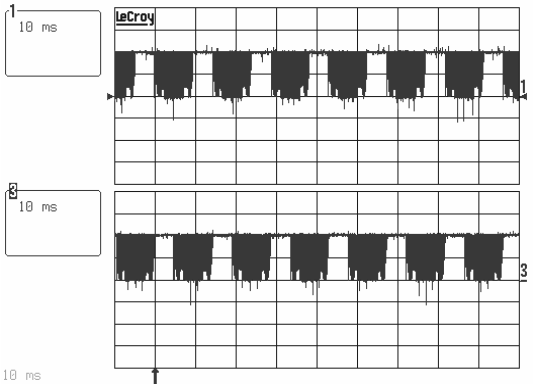

Figure 18. Voltage of phase A and phase B (V_{an} and V_{bn}); DC link voltage: 375V, motor speed: 1500rpm; V_{ref}: 3.1V.

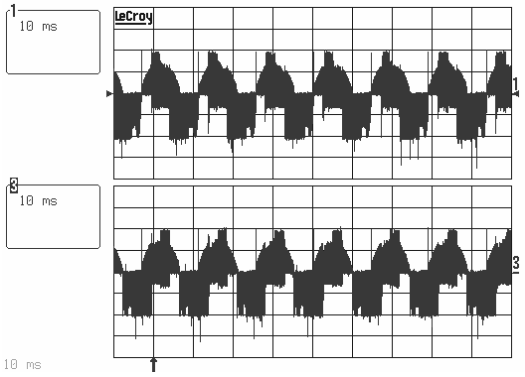

Figure 19. V_{ac} and V_{bc}; DC link voltage: 375V, motor speed: 1500rpm; V_{ref}: 3.1V.

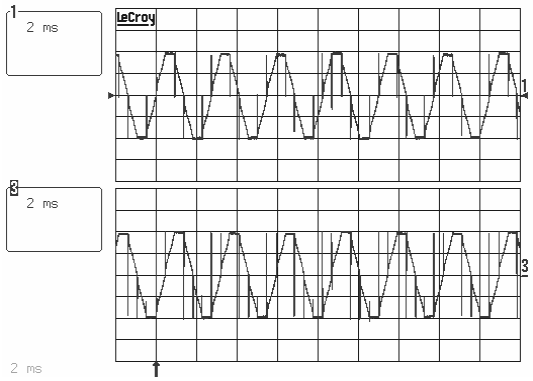

Figure 20. V_{ac} and V_{bc}; DC link voltage: 375V, motor speed: 5000rpm, V_{ref}: 10V.

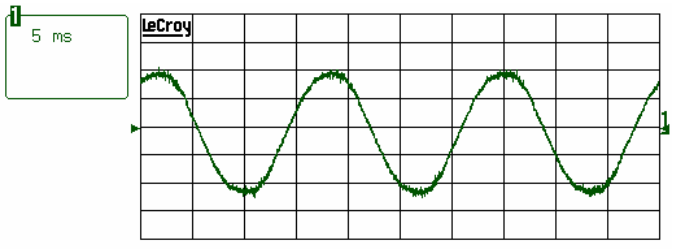

Figure 21. Supply current waveform using the NCP1650, 2.5A/div.

Operational performance characteristics of the machine with different loads have been tested comprehensively. The following measurements have been done when the motor was operating at 1500rpm and rated torque of 3.2 N-m. The motor was loaded by a magnetic brake in our laboratory.

- RMS supply current: 3.4A
- RMS supply voltage: 220VAC/60Hz
- Measured power factor: 0.83 lagging
- Measured total harmonic distortion (THD): 5%
- Efficiency: 78.5%

Table I presents final test results of the motor drive system during the final competition at Advanced Energy, Raleigh, NC, May 20-23, 2003. This system performed superior and was the only system completing most of the tests including the overnight durability test. Figures 22 and 23 show IIT's motor drive system under test at the final competition site.

TABLE I. FINAL TEST RESULTS AT THE COMPETITION SITE.

Speed Reference	Load	Input Power (W)	Speed (rpm)	Speed Ripple (%)	Efficiency (%)
150 rpm	No Load (0.19Nm)	20.79	152.75	1.83	14.79
150 rpm	35W	110.73	138.14	7.91	32.39
450 rpm	No Load (0.30Nm)	36.40	454.80	1.07	38.99
450 rpm	2.00Nm	152.62	443.88	1.36	61.30
450 rpm	3.18Nm	251.67	436.70	2.96	57.40
750 rpm	No Load (0.31Nm)	49.51	752.93	0.39	48.91
750 rpm	2.00Nm	221.37	740.98	1.20	70.71
750 rpm	3.18Nm	360.59	732.97	2.27	67.75
1050 rpm	No Load (0.39Nm)	75.45	1051.19	0.11	58.70
1050 rpm	2.00Nm	291.49	1038.90	1.06	75.78
1050 rpm	3.18Nm	462.94	1030.43	1.86	74.32
1500 rpm	2.00Nm	399.81	1483.07	1.13	80.99
1500 rpm	3.18Nm	625.19	1473.51	1.77	78.54
1500 rpm	500W	637.82	1473.14	1.79	78.46
1500 rpm	350W	435.75	1486.59	0.89	80.07
1500 rpm	250W	310.57	1489.86	0.68	81.19
1500 rpm	150W	195.07	1491.30	0.58	77.82
1500 rpm	50W	81.92	1497.59	0.02	61.84
1500 rpm	No Load (0.26Nm)	76.76	1498.95	0.01	53.35
2500 rpm	500W	597.84	2488.38	0.46	83.72
3500 rpm	500W	597.66	3490.16	0.28	83.92
5000 rpm	No Load (0.38Nm)	256.65	4276.99	14.46	67.14
5000 rpm	500W	607.33	3991.46	20.17	83.17

V. CONCLUSION

In this paper, the permanent magnet brush-less DC motor and its power electronic drive designed and developed for the 2003 IEEE/DOE/DOD International Future Energy Challenge by IIT's student team were presented. The main goal of IIT's

team was to implement a low-cost, high-performance design with the capability of handling different competition tests. The system was designed to operate from a single-phase residential source (240V, 50Hz) and was tested with a 220V, 60Hz source. In order to achieve a very low-cost system, no digital signal processor, microprocessor, or microcontroller was used. Instead, the team was able to successfully develop the system meeting the requirements of the challenge using several ICs. This, in turn, has significant advantages for mass production because of the economical development, simplicity, reliability, and ease of manufacturing.

Figure 22. IIT's motor drive system under test at Advanced Energy, Raleigh, NC, May 2003.

Figure 23. IIT's motor drive system under the overnight durability test at Advanced Energy, Raleigh, NC, May 2003.

ACKNOWLEDGEMENT

Student team members were Mr. Aly A. Aboulnaga (Ph.D. EE), Mr. Piyush C. Desai (M.S. EE), Mr. Anthony Villagomez (B.S. EE), Mr. Fernando Rodriguez (B.S./M.S. EE), Mr. Timothy Cooke (B.S./M.S. EE/CPE), Mr. Jeffrey Szekely (B.S. EE/CPE), Ms. Marina Kramskaya (B.S. EE), Ms. Valliy K. Dawood (B.S. EE), Mr. Hani Bodak (B.S. EE), Mr. Mark Ihimoyan (B.S. EE/CPE), Ms. Sahar Kohanim (B.S. Chemistry), and Mr. Loren McDaniel (B.S./M.S. ME). They are gratefully acknowledged.

Other than the laboratory facilities, the Grainger Power Electronics and Motor Drives Laboratory at IIT has provided main funds to help secure special parts and equipment. The student team also contacted potential sponsors to secure outside sponsorship. Sponsorship of the following companies for this work is gratefully acknowledged: Advanced Magnetic Products, Allegro Microsystems Incorporated, Ansoft Corporation, API Delevan, Bodine Electric Company, C&D Technologies, Inc., Coilcraft, Inc., Fairchild Semiconductor, Infranor Inc., International Rectifier, IXYS Corporation, Mills Electric Co., MPC Products Corporation, NJR Corporation, ON Semiconductor, Poly-Scientific, Northrop Grumman Component Technologies, Inc., and ST Microelectronics.

We would also like to thank Mr. Craig Scott and MPC Products Corporation, Skokie, Illinois as well as Mills Electric Co. of Indiana for the technical assistance and providing the team their machine manufacturing facility, which have been extremely helpful in fabricating the designed BLDC motor. Support of Mr. James E. Marth, Bodine Electric Company, Chicago, Illinois is also gratefully acknowledged. We would also like to thank Mr. John Carbone and Infranor Inc., Naugatuck, Connecticut for their support and final motor for the competition.

REFERENCES

[1] Electronic Motor Drives 2001-2005, Report #1202, Drives Research Corporation, August 2001.

[2] Consortium for Energy Efficiency (CEE), http://www.cee1.org/

[3] John C. Andreas, *Energy Efficient Electric Motors: Selection and Applications,* Marcel Dekker, Inc., 1992.

[4] D. H. Hart, *Introduction to Power Electronics*, Prentice-Hall, 1997.

[5] P. T. Krein, *Elements of Power Electronics*, Oxford University Press, 1998.

[6] N. Mohan, T. M. Undeland, and W. P. Robbins, *Power Electronics: Converters, Applications, and Design*, John Wiley & Sons, 1995.

[7] M. H. Rashid, *Power Electronics,* 2nd Edition, Prentice Hall, 1993.

[8] T. L. Skvarenina, *The Power Electronics Handbook,* CRC Press, 2002.

[9] R. Krishnan, *Electric Motor Drives: Modeling, Analysis, and Control*, Prentice-Hall, 2001.

[10] B. K. Bose, *Modern Power Electronics and AC Drives,* Prentice Hall PTR, 2002.

[11] J. G. Kassakian, M. F. Schlecht, and G. C. Verghese, *Principles of Power Electronics,* Addison Wesley, 1991.

[12] A. M. Trzynadlowski, *Introduction to Modern Power Electronics,* John Wiley and Sons, 1998.

[13] J. F. Gieras and M. Wind, *Permanent Magnet Motor Technology: Design and Applications,* Second Edition, Marcel Dekker Inc., New York Basel.

[14] *Maxwell 2D Manual,* Ansoft Corporation.